J. Plasma Phys. (2021), *vol.* 87, 905870310 © The Author(s), 2021.
Published by Cambridge University Press
doi:10.1017/S0022377821000593

General dispersion properties of magnetized plasmas with drifting bi-Kappa distributions. DIS-K: Dispersion Solver for Kappa Plasmas

R.A. López[1,†], **S.M. Shaaban**[2,3] **and M. Lazar**[4,5]

[1]Departamento de Física, Universidad de Santiago de Chile, Usach, 9170124 Santiago, Chile

[2]Institute of Experimental and Applied Physics, University of Kiel, Leibnizstrasse 11, D-24118 Kiel, Germany

[3]Theoretical Physics Research Group, Physics Department, Faculty of Science, Mansoura University, 35516 Mansoura, Egypt

[4]Centre for Mathematical Plasma Astrophysics, KU Leuven, Celestijnenlaan 200B, B-3001 Leuven, Belgium

[5]Institut für Theoretische Physik, Lehrstuhl IV: Weltraum- und Astrophysik, Ruhr-Universität Bochum, D-44780 Bochum, Germany

(Received 24 February 2021; revised 6 May 2021; accepted 18 May 2021)

Space plasmas are known to be out of (local) thermodynamic equilibrium, as observations show direct or indirect evidences of non-thermal velocity distributions of plasma particles. Prominent are the anisotropies relative to the magnetic field, anisotropic temperatures, field-aligned beams or drifting populations, but also, the suprathermal populations enhancing the high-energy tails of the observed distributions. Drifting bi-Kappa distribution functions can provide a good representation of these features and enable for a kinetic fundamental description of the dispersion and stability of these collision-poor plasmas, where particle–particle collisions are rare but wave–particle interactions appear to play a dominant role in the dynamics. In the present paper we derive the full set of components of the dispersion tensor for magnetized plasma populations modelled by drifting bi-Kappa distributions. A new solver called DIS-K (DIspersion Solver for Kappa plasmas) is proposed to solve numerically the dispersion relations of high complexity. The solver is validated by comparing with the damped and unstable wave solutions obtained with other codes, operating in the limits of drifting Maxwellian and non-drifting Kappa models. These new theoretical tools enable more realistic characterizations, both analytical and numerical, of wave fluctuations and instabilities in complex kinetic configurations measured in-situ in space plasmas.

Key words: plasma waves, plasma instabilities, space plasma physics

1. Introduction

In collision-poor plasmas from the heliosphere, in-situ measurements of the velocity distributions of particles reveal a variety of non-thermal features, such as suprathermal

† Email address for correspondence: rlopez186@gmail.com

populations and anisotropies with respect to the magnetic field direction, mainly anisotropic temperatures and field-aligned beams (Maksimovic *et al.* 2005; Marsch 2006; Wilson *et al.* 2019*a*). Physical mechanisms that can maintain these states of non-equilibrium are mainly triggered by the small-scale (kinetic) wave turbulence and fluctuations, which are also confirmed by observations (Alexandrova *et al.* 2013). If resonant wave–particle interactions can preferentially energize plasma particles leading to kinetic anisotropies (Isenberg & Vasquez 2019), stochastic acceleration by plasma turbulence may generate more diffuse suprathermal populations enhancing the high-energy tails of velocity distributions (Bian *et al.* 2014). The same wave–particle interactions are also responsible for the excitation of instabilities (Wilson *et al.* 2013; Bowen *et al.* 2020), or further relaxation of anisotropic particles under the diffusion effect of the enhanced fluctuations (Bale *et al.* 2009; Tong *et al.* 2019). These fluctuations are mainly powered by the solar outflows inducing large-scale perturbations and wave turbulence, which are transported by the expanding solar wind, and decay nonlinearly toward smaller (kinetic) scales where a perpetual exchange of energy between plasma waves and particles ultimately takes place (Leamon *et al.* 1999; Verscharen, Klein & Maruca 2019*a*, and references therein). Representative are not only the mechanisms of resonant dissipation (damping) of waves leading to the heating of particles, but also the instabilities that can transfer (free) energy from anisotropic and suprathermal particles to waves and fluctuations (Lazar *et al.* 2019; Shaaban *et al.* 2019; Verscharen *et al.* 2019*b*; Shaaban, Lazar & Schlickeiser 2021*b*).

Locally, small-scale fluctuations can be markedly enhanced by the kinetic instabilities, sometimes rather than a turbulent cascade (Gary *et al.* 2016; Tong *et al.* 2019; Woodham *et al.* 2019). However, in the absence of energetic events (e.g. flares or coronal mass ejections) the wave fluctuations measured in-situ in space plasmas have wide bandwidths and small amplitudes, such that, their properties and effects on particles can be addressed in the frame of linear and quasilinear (known as QL) theories (Gary 1993; Gary *et al.* 2016; Yoon 2017, 2019). However, if the fluctuations are a superposition of nonlinear structures or fluid-like turbulent eddies, then linear and quasilinear theory do not apply. Revealing these linear and quasilinear properties of waves and instabilities in the solar wind, already perceived as a truly natural laboratory, has therefore acquired a special motivation. To do that, we need to derive the dispersion and stability relations, and, implicitly, the dielectric tensor of the plasma system relying directly on the shape of underlying velocity distributions (Stix 1992). The observed velocity distributions of plasma particles combine kinetic anisotropies, relative to the magnetic field direction, e.g. anisotropic temperatures (Kasper *et al.* 2003; Štverák *et al.* 2008) or field aligned beams (Pilipp *et al.* 1987; Marsch 2006), and suprathermal tails well reproduced by the Kappa distribution functions (Pierrard & Lazar 2010; Lazar *et al.* 2017). The picture can be clarified by pointing out the details in the velocity distributions. For instance, the electrons show a low-energy core, well reproduced by a bi-Maxwellian distribution function, a suprathermal halo and an electron strahl, both of them well described by bi-Kappa distribution functions with relative drifts parallel to the magnetic field (Maksimovic *et al.* 2005; Lazar *et al.* 2017; Wilson *et al.* 2019*a*,*b*). The relative drift between core and halo is in general modest (Wilson *et al.* 2019*a*) allowing the incorporation of these two components by another bi-Kappa, which is nearly bi-Maxwellian at low energies but decreases as a power law at high energies (Vasyliunas 1968; Lazar *et al.* 2017). It is thus obvious that Kappa models, including anisotropic variants like bi-Kappa, with or without relative drifts, are widely invoked for their success in modelling the observed distributions, not only for electrons, but also for protons and heavier ions (Collier *et al.* 1996; Pierrard & Lazar 2010; Mason & Gloeckler 2012).

Despite these observational evidences, in the dispersion and stability analysis the velocity distributions are still reduced to idealized bi-Maxwellian representations (Verscharen *et al.* 2019*b*; López *et al.* 2020; Shaaban & Lazar 2020; Shaaban *et al.* 2021*a*), for which the dielectric tensor is already explicitly derived (Stix 1992). In the context of drifting bi-Kappa plasmas, the analysis so far is limited only to the propagation parallel to the magnetic field (Shaaban, Lazar & Poedts 2018; Shaaban *et al.* 2020), because the complete expression of the dielectric tensor, and, implicitly, the general dispersion relation for an arbitrary direction of propagation, are not trivial, but rather complicated, and have not been derived yet. Therefore, numerical solvers capable of resolving the full spectrum of waves and instabilities of this configuration do not yet exist. In the present paper we provide the full expression of the dielectric tensor and general dispersion relation for magnetized plasma particles described by drifting bi-Kappa distribution functions. Thus it becomes possible for an advanced analysis to characterize, in a more realistic manner, the dispersion and stability of plasma populations revealed by the in-situ observations. For instance, the suprathermal halo, and strahl electrons carrying the main heat flux in the solar wind (Lazar *et al.* 2020*a*), whose evolution with increasing the heliospheric distance (Hammond *et al.* 1996; Maksimovic *et al.* 2005) are expected to be controlled by the self-generated instabilities (Verscharen *et al.* 2019*b*; Jeong *et al.* 2020; López *et al.* 2020; Micera *et al.* 2020).

Also reported here is a new generalized Dispersion Solver for Kappa-distributed plasmas (abbreviated DIS-K), which implements the new dispersion tensor and numerically resolves the dispersion and (in)stability properties for all directions of propagation with respect to the magnetic field. Chronologically speaking, the first numerical solvers were built for Maxwellian plasmas, such as WHAMP (Roennmark 1982) and PLADAWAN (Viñas, Wong & Klimas 2000), or the more recent variants, PLUME (Klein & Howes 2015) and NDHS (Verscharen & Chandran 2018). Progress has also been made for other models, such as the Kappa distribution, which introduces new analytical and numerical challenges. Of major importance were the detailed studies of the new dispersion function for Kappa distributions (Summers & Thorne 1991; Mace & Hellberg 1995), on which most of the codes developed later are based. Initially, efforts were dedicated to unmagnetized plasmas or reduced configurations in magnetized plasmas, such as electrostatic approximation or parallel propagation (Hellberg & Mace 2002; Lazar & Poedts 2009; Viñas *et al.* 2017). Earlier approaches to describe perpendicular and oblique propagation (Summers, Xue & Thorne 1994; Cattaert, Hellberg & Mace 2007; Basu 2009) have more recently been complemented by rigorous mathematical calculations of the general dielectric tensor providing compact and closed forms of its components (Liu *et al.* 2014; Gaelzer & Ziebell 2016; Gaelzer, Ziebell & Meneses 2016; Kim *et al.* 2017). A relatively recent numerical implementation of the dielectric tensor for non-drifting bi-Kappa plasmas is DHSARK (Astfalk, Görler & Jenko 2015), a pioneer solver for studying kinetic electromagnetic instabilities (Astfalk 2018). Other similar codes (not named yet) were also developed in the last few years, in order to extend the spectral analysis in bi-Kappa plasmas (Lazar *et al.* 2019; López *et al.* 2019), and pave the way for a more elaborated tool, as our new solver DIS-K. In this paper we present the first numerical results obtained with this solver, which is capable of resolving more complex dispersion relations for plasma populations with drifting bi-Kappa populations, and the full spectrum of stable or unstable modes, of any nature, e.g. electrostatic or electromagnetic, periodic or aperiodic.

Our paper is organized as follows. In § 2 we start by introducing the general (linear) dispersion tensor, and the drifting bi-Kappa parameterization for a plasma of electrons and ions. Explicit expressions of the newly derived components of the dispersion tensor are

https://doi.org/10.1017/S0022377821000593 Published online by Cambridge University Press

presented in § 3. We also show the agreement with different limit cases, e.g. Maxwellian, and non-drifting bi-Kappa, from previous studies. In § 4 we solve numerically the dispersion relation for some illustrative cases specific to these limits, which allows us to compare with the previous results and test our numerical solver. Finally, our results are summarized in § 5.

2. Theoretical formalism

Space plasmas are subject to multiple sources of inhomogeneities and temporal variations, such as wave turbulence, the interaction of fast and slow streams, or even the solar wind expansion. However, to describe the small-scale wave fluctuations and instabilities we can assume these plasmas are sufficiently homogeneous, especially because linear and quasilinear theories seem to explain quite well the kinetic properties of plasma particles revealed by in-situ observations (Kasper *et al.* 2003; Štverák *et al.* 2008; Verscharen *et al.* 2019*a*). These are waves and instabilities which mainly depend on the nature of particle velocity distributions, and their analysis requires a kinetic approach.

2.1. *General dispersion relation*

Without loss of generality we assume Cartesian coordinates (x, y, z) with the z axis parallel to the magnetic field $\boldsymbol{B}$, and with the wavevector $\boldsymbol{k}$ in the $(x\text{–}z)$ plane, such that

$$\boldsymbol{k} = k_\perp \hat{\boldsymbol{x}} + k_\parallel \hat{\boldsymbol{z}}, \tag{2.1}$$

where $\parallel, \perp$ are defined with respect to the magnetic field direction. From the Vlasov–Maxwell equations one can derive the general expression of the dispersion relation (Stix 1992)

$$\boldsymbol{\Lambda} \cdot \boldsymbol{E} = 0 \tag{2.2}$$

in terms of the electric field of the wave fluctuation $\boldsymbol{E}(\boldsymbol{k}, \omega)$ and the dispersion tensor $\boldsymbol{\Lambda}$. For arbitrary (but still gyrotropic) velocity distribution functions $F_a(v_\perp, v_\parallel)$ of plasma species of sort a (e.g. $a = e, p, i$ for electrons, protons and ions, respectively) the components of the dispersion read as follows:

$$\begin{aligned} \Lambda_{ij}(\boldsymbol{k}, \omega) = \delta_{ij} - \frac{c^2k^2}{\omega^2}\left(\delta_{ij} - \frac{k_ik_j}{k^2}\right) \\ + \sum_a \frac{\omega_{\mathrm{pa}}^2}{\omega^2}\int \mathrm{d}\boldsymbol{v} \sum_{n=-\infty}^{\infty} \frac{V_i^n V_j^{n*}}{\omega - k_\parallel v_\parallel - n\Omega_a}\left(\frac{\omega - k_\parallel v_\parallel}{v_\perp}\frac{\partial F_a}{\partial v_\perp} + k_\parallel \frac{\partial F_a}{\partial v_\parallel}\right) \\ + \hat{\boldsymbol{B}}_i\hat{\boldsymbol{B}}_j \sum_a \frac{\omega_{\mathrm{pa}}^2}{\omega^2}\int \mathrm{d}\boldsymbol{v}\, v_\parallel \left(\frac{\partial F_a}{\partial v_\parallel} - \frac{v_\parallel}{v_\perp}\frac{\partial F_a}{\partial v_\perp}\right). \end{aligned} \tag{2.3}$$

Here

$$\boldsymbol{V}^n = v_\perp \frac{n\mathrm{J}_n(b)}{b}\hat{\boldsymbol{e}}_1 - \mathrm{i}v_\perp \mathrm{J}_n'(b)\hat{\boldsymbol{e}}_2 + v_\parallel \mathrm{J}_n(b)\hat{\boldsymbol{e}}_3, \quad \hat{\boldsymbol{B}} = \boldsymbol{B}/B = \hat{\boldsymbol{e}}_3, \quad b = \frac{k_\perp v_\perp}{\Omega_a}, \tag{2.4a–c}$$

where $\mathrm{J}_n(b)$ is the Bessel function with $\mathrm{J}_n'(b)$ its first derivative, i is the imaginary unit, c is the speed of light, $\omega_{\mathrm{pa}} = \sqrt{4\pi n_a q_a^2/m_a}$ is the plasma frequency, $\Omega_a = q_a B_0/(m_a c)$ the gyrofrequency, q_a the charge, m_a the mass and n_a the number density of species a, respectively.

https://doi.org/10.1017/S0022377821000593 Published online by Cambridge University Press

2.2. *Drifting bi-Kappa distribution*

For magnetized plasma particles in space environments, realistic models able to reproduce the main departures from thermal equilibrium, i.e. anisotropies and suprathermal populations, are drifting bi-Kappa velocity distribution functions

$$F_a(v_\perp, v_\parallel) = \frac{1}{\pi^{3/2}} \frac{1}{\alpha_{\perp a}^2 \alpha_{\parallel a}} \frac{\Gamma(\kappa_a+1)}{\kappa_a^{3/2}\Gamma(\kappa_a-1/2)} \left[1 + \frac{(v_\parallel - U_a)^2}{\kappa_a \alpha_{\parallel a}^2} + \frac{v_\perp^2}{\kappa_a \alpha_{\perp a}^2}\right]^{-\kappa_a-1}, \tag{2.5}$$

where κ_a is the power law index, $\Gamma(x)$ is the Gamma function, U_a is the drift speed, and the parameters $\alpha_{\parallel,\perp}$, known as the most probable speed (Vasyliunas 1968),

$$\alpha_{\parallel a} = \left(\frac{2k_B T_{\parallel a}}{m_a}\right)^{1/2}, \quad \alpha_{\perp a} = \left(\frac{2k_B T_{\perp a}}{m_a}\right)^{1/2}, \tag{2.6a,b}$$

correspond to the thermal speeds of the Maxwellian limit that approximately describe the low-energy core out of the Kappa distribution (Lazar, Poedts & Fichtner 2015; Lazar, Fichtner & Yoon 2016). Here k_B is the Boltzmann's constant. The thermal speeds are related to the kinetic temperature through the second-order moment of the distribution,

$$T_{\parallel a}^{(\kappa)} = \int \mathrm{d}\boldsymbol{v}(v_\parallel - U_a)^2 F_a(v_\perp, v_\parallel) = \frac{m_a}{2k_B} \frac{2\kappa_a}{2\kappa_a - 3} \alpha_{\parallel a}^2, \tag{2.7}$$

$$T_{\perp a}^{(\kappa)} = \int \mathrm{d}\boldsymbol{v}\, v_\perp^2 F_a(v_\perp, v_\parallel) = \frac{m_a}{2k_B} \frac{2\kappa_a}{2\kappa_a - 3} \alpha_{\perp a}^2, \tag{2.8}$$

requiring $\kappa_a > 3/2$. These kinetic temperatures are greater than the corresponding temperatures of the Maxwellian limit, introduced in (2.6a,b), through $T_{\parallel,\perp} = \lim_{\kappa\to\infty} T_{\parallel,\perp}^{(\kappa)} < T_{\parallel,\perp}^{(\kappa)}$.

3. Dispersion tensor

We substitute the drifting bi-Kappa distribution function (2.5) in the general expression (2.3) of the dispersion tensor, and after integration obtain for each element of the dispersion tensor the following expressions:

$$\Lambda_{ij} = \begin{pmatrix} D_{11} & \mathrm{i}D_{12} & D_{13} \\ -\mathrm{i}D_{12} & D_{22} & \mathrm{i}D_{23} \\ D_{13} & -\mathrm{i}D_{23} & D_{33} \end{pmatrix}_{ij}, \tag{3.1}$$

$$D_{11} = 1 - \frac{c^2 k_\parallel^2}{\omega^2} + \sum_a \frac{\omega_{\mathrm{pa}}^2}{\omega^2} \sum_{n=-\infty}^{\infty} \frac{n^2}{\lambda_a} \left[\xi_a Z_{n,\kappa}^{(1,2)}(\lambda_a, \zeta_a^n) + \frac{A_a}{2} \frac{\partial}{\partial \zeta_a^n} Z_{n,k}^{(1,1)}(\lambda_a, \zeta_a^n)\right], \tag{3.2}$$

$$D_{22} = 1 - \frac{c^2 k^2}{\omega^2} + \sum_a \frac{\omega_{\mathrm{pa}}^2}{\omega^2} \sum_{n=-\infty}^{\infty} \left[\xi_a W_{n,\kappa}^{(1,2)}(\lambda_a, \zeta_a^n) + \frac{A_a}{2} \frac{\partial}{\partial \zeta_a^n} W_{n,k}^{(1,1)}(\lambda_a, \zeta_a^n)\right], \tag{3.3}$$

$$D_{12} = \sum_a \frac{\omega_{\mathrm{pa}}^2}{\omega^2} \sum_{n=-\infty}^{\infty} n \left[\xi_a \frac{\partial}{\partial \lambda_a} Z_{n,\kappa}^{(1,2)}(\lambda_a, \zeta_a^n) + \frac{A_a}{2} \frac{\partial^2}{\partial \lambda_a \partial \zeta_a^n} Z_{n,k}^{(1,1)}(\lambda_a, \zeta_a^n)\right], \tag{3.4}$$

$$D_{13} = \frac{c^2 k_\perp k_\parallel}{\omega^2} + 2 \sum_a \frac{q_a}{|q_a|} \frac{\omega_{\mathrm{pa}}^2}{\omega^2} \sqrt{\frac{T_{\parallel a}}{T_{\perp a}}} \frac{U_a}{\alpha_{\parallel a}} \sum_{n=-\infty}^{\infty} \frac{n}{\sqrt{2\lambda_a}} \xi_a Z_{n,\kappa}^{(1,2)}(\lambda_a, \zeta_a^n)$$

https://doi.org/10.1017/S0022377821000593 Published online by Cambridge University Press

$$-\sum_a \frac{q_a}{|q_a|}\frac{\omega_{pa}^2}{\omega^2}\sqrt{\frac{T_{\parallel a}}{T_{\perp a}}}\sum_{n=-\infty}^{\infty}\frac{n}{\sqrt{2\lambda_a}}\left[\xi_a - A_a\left(\zeta_a^n + \frac{U_a}{\alpha_{\parallel a}}\right)\right]\frac{\partial}{\partial\zeta_a^n}Z_{n,\kappa}^{(1,1)}(\lambda_a,\zeta_a^n), \tag{3.5}$$

$$D_{23} = \sum_a \frac{\omega_{pa}^2}{\omega^2}\frac{|q_a|}{q_a}\sqrt{\frac{T_{\parallel a}}{T_{\perp a}}}\sqrt{\frac{\lambda_a}{2}}\sum_{n=-\infty}^{\infty}\left[\xi_a - A_a\left(\zeta_a^n + \frac{U_a}{\alpha_{\parallel a}}\right)\right]\frac{\partial^2}{\partial\lambda_a\partial\zeta_a^n}Z_{n,\kappa}^{(1,1)}(\lambda_a,\zeta_a^n)$$

$$-2\sum_a \frac{\omega_{pa}^2}{\omega^2}\frac{|q_a|}{q_a}\sqrt{\frac{T_{\parallel a}}{T_{\perp a}}}\sqrt{\frac{\lambda_a}{2}}\frac{U_a}{\alpha_{\parallel a}}\sum_{n=-\infty}^{\infty}\xi_a\frac{\partial}{\partial\lambda_a}Z_{n,\kappa}^{(1,2)}(\lambda_a,\zeta_a^n), \tag{3.6}$$

$$D_{33} = 1 - \frac{c^2k_\perp^2}{\omega^2} + 2\sum_a \frac{\omega_{pa}^2}{\omega^2}\frac{T_{\parallel a}}{T_{\perp a}}\left(1-\frac{1}{2\kappa_a}\right)\frac{U_a^2}{\alpha_{\parallel a}^2} + 2\sum_a \frac{\omega_{pa}^2}{\omega^2}\frac{T_{\parallel a}}{T_{\perp a}}\frac{U_a^2}{\alpha_{\parallel a}^2}\sum_{n=-\infty}^{\infty}\xi_a Z_{n,\kappa}^{(1,2)}(\lambda_a,\zeta_a^n)$$

$$-\sum_a \frac{\omega_{pa}^2}{\omega^2}\frac{T_{\parallel a}}{T_{\perp a}}\sum_{n=-\infty}^{\infty}\left[(\xi_a - A_a\zeta_a^n)\left(\zeta_a^n + 2\frac{U_a}{\alpha_{\parallel a}}\right) - A_a\frac{U_a^2}{\alpha_{\parallel a}^2}\right]\frac{\partial}{\partial\zeta_a^n}Z_{n,\kappa}^{(1,1)}(\lambda_a,\zeta_a^n). \tag{3.7}$$

Here we have used the following definitions (Gaelzer & Ziebell 2016; Gaelzer *et al.* 2016; Kim *et al.* 2017):

$$Z_{n,\kappa}^{(\alpha,\beta)}(\lambda,\xi) = 2\int_0^\infty \mathrm{d}x\,\frac{x\mathrm{J}_n^2(x\sqrt{2\lambda})}{(1+x^2/\kappa)^{\kappa+\alpha+\beta-1}}Z_\kappa^{(\alpha,\beta)}\left(\frac{\xi}{\sqrt{1+x^2/\kappa}}\right), \tag{3.8}$$

$$\mathrm{Y}_{n,\kappa}^{(\alpha,\beta)}(\lambda,\xi) = \frac{2}{\lambda}\int_0^\infty \mathrm{d}x\,\frac{x^3\mathrm{J}_{n-1}(x\sqrt{2\lambda})\mathrm{J}_{n+1}(x\sqrt{2\lambda})}{(1+x^2/\kappa)^{\kappa+\alpha+\beta-1}}Z_\kappa^{(\alpha,\beta)}\left(\frac{\xi}{\sqrt{1+x^2/\kappa}}\right), \tag{3.9}$$

$$W_{n,\kappa}^{(\alpha,\beta)}(\lambda,\xi) = \frac{n^2}{\lambda}Z_{n,\kappa}^{(\alpha,\beta)}(\lambda,\xi) - 2\lambda\mathrm{Y}_{n,\kappa}^{(\alpha,\beta)}(\lambda,\xi), \tag{3.10}$$

$$Z_\kappa^{(\alpha,\beta)}(\xi) = \frac{1}{\pi^{1/2}\kappa^{\beta+1/2}}\frac{\Gamma(\kappa+\alpha+\beta-1)}{\Gamma(\kappa+\alpha-3/2)}\int_{-\infty}^{\infty}\mathrm{d}s\,\frac{(1+s^2/\kappa)^{-(\kappa+\alpha+\beta-1)}}{s-\xi}, \tag{3.11}$$

$$\lambda_a = \frac{k_\perp^2\alpha_{\perp a}^2}{2\Omega_a^2}, \tag{3.12}$$

$$\xi_a = \frac{\omega - k_\parallel U_a}{k_\parallel \alpha_{\parallel a}}, \tag{3.13}$$

$$\zeta_a^n = \frac{\omega - k_\parallel U_a - n\Omega_a}{k_\parallel\alpha_{\parallel a}}, \tag{3.14}$$

$$A_a = 1 - \frac{T_{\perp a}}{T_{\parallel a}}. \tag{3.15}$$

A list of the specific expressions required in (3.2)–(3.7) are provided in Appendices A and B.

From (2.2), the dispersion relation for non-trivial solutions ($E \neq 0$) requires the determinant of the dispersion tensor to satisfy $\det\{\boldsymbol{\Lambda}\} = 0$, which can be written explicitly as

$$0 = D_{11}D_{22}D_{33} - D_{11}D_{23}^2 - D_{22}D_{13}^2 - D_{33}D_{12}^2 - 2D_{12}D_{13}D_{23}. \tag{3.16}$$

In order to optimize the performance of the dispersion solver, we can further simplify the expressions of the dispersion tensor components in (3.2)–(3.7), to minimize the number of integrals that need to be performed. These components can be written as follows:

$$D_{11} = 1 - \frac{c^2 k_\parallel^2}{\omega^2} + \sum_a \frac{\omega_{pa}^2}{\omega^2} \sum_{n=-\infty}^{\infty} \frac{n^2}{\lambda_a} \mathrm{I}_{11}(\lambda_a, \zeta_a^n), \tag{3.17}$$

$$D_{22} = 1 - \frac{c^2 k^2}{\omega^2} + \sum_a \frac{\omega_{pa}^2}{\omega^2} \sum_{n=-\infty}^{\infty} \mathrm{I}_{22}(\lambda_a, \zeta_a^n), \tag{3.18}$$

$$D_{12} = \sum_a \frac{\omega_{pa}^2}{\omega^2} \sum_{n=-\infty}^{\infty} n\mathrm{I}_{12}(\lambda_a, \zeta_a^n), \tag{3.19}$$

$$D_{13} = \frac{c^2 k_\perp k_\parallel}{\omega^2} + \sum_a \frac{q_a}{|q_a|} \frac{\omega_{pa}^2}{\omega^2} \sqrt{\frac{T_{\parallel a}}{T_{\perp a}}} \sum_{n=-\infty}^{\infty} \frac{n}{\sqrt{2\lambda_a}} \mathrm{I}_{13}(\lambda_a, \zeta_a^n), \tag{3.20}$$

$$D_{23} = \sum_a \frac{|q_a|}{q_a} \frac{\omega_{pa}^2}{\omega^2} \sqrt{\frac{T_{\parallel a}}{T_{\perp a}}} \sqrt{\frac{\lambda_a}{2}} \sum_{n=-\infty}^{\infty} \mathrm{I}_{23}(\lambda_a, \zeta_a^n), \tag{3.21}$$

$$D_{33} = 1 - \frac{c^2 k_\perp^2}{\omega^2} + 2\sum_a \frac{\omega_{pa}^2}{\omega^2} \frac{T_{\parallel a}}{T_{\perp a}} \left(1 - \frac{1}{2\kappa_a}\right) \frac{U_a^2}{\alpha_{\parallel a}^2} + 2\sum_a \frac{\omega_{pa}^2}{\omega^2} \frac{T_{\parallel a}}{T_{\perp a}} \sum_{n=-\infty}^{\infty} \mathrm{I}_{33}(\lambda_a, \zeta_a^n). \tag{3.22}$$

Now, each component of the dispersion tensor depends on a single integral of the form

$$\mathrm{I}_{11}(\lambda_a, \zeta_a^n) = \int_0^\infty \mathrm{d}x \, \frac{2x\mathrm{J}_n^2(x\sqrt{2\lambda_a})}{(1 + x^2/\kappa_a)^{\kappa_a + 3/2}} H_a^n(x), \tag{3.23}$$

$$\mathrm{I}_{22}(\lambda_a, \zeta_a^n) = \int_0^\infty \mathrm{d}x \, \frac{2x\left(\dfrac{n^2}{\lambda_a}\mathrm{J}_n^2\left(x\sqrt{2\lambda_a}\right) - 2x^2 \mathrm{J}_{n-1}\left(x\sqrt{2\lambda_a}\right)\mathrm{J}_{n+1}\left(x\sqrt{2\lambda_a}\right)\right)}{(1 + x^2/\kappa_a)^{\kappa + 3/2}} H_a^n(x), \tag{3.24}$$

$$\mathrm{I}_{12}(\lambda_a, \zeta_a^n) = \sqrt{\frac{2}{\lambda_a}} \int_0^\infty \mathrm{d}x \, \frac{x^2 \mathrm{J}_n\left(x\sqrt{2\lambda_a}\right)\left[\mathrm{J}_{n-1}\left(x\sqrt{2\lambda_a}\right) - \mathrm{J}_{n+1}\left(x\sqrt{2\lambda_a}\right)\right]}{(1 + x^2/\kappa)^{\kappa + 3/2}} H_a^n(x), \tag{3.25}$$

$$\mathrm{I}_{13}(\lambda_a, \zeta_a^n) = 4\int_0^\infty \mathrm{d}x \, \frac{x\mathrm{J}_n^2(x\sqrt{2\lambda_a})}{(1 + x^2/\kappa_a)^{\kappa_a + 3/2}} \mathrm{K}_a^n(x), \tag{3.26}$$

$$\mathrm{I}_{23}(\lambda_a, \zeta_a^n) = -\frac{4}{\sqrt{2\lambda_a}} \int_0^\infty \mathrm{d}x \, \frac{x^2 \mathrm{J}_n\left(x\sqrt{2\lambda_a}\right)\left[\mathrm{J}_{n-1}\left(x\sqrt{2\lambda_a}\right) - \mathrm{J}_{n+1}\left(x\sqrt{2\lambda_a}\right)\right]}{(1 + x^2/\kappa_a)^{\kappa_a + 3/2}} \mathrm{K}_a^n(x), \tag{3.27}$$

$$\mathrm{I}_{33}(\lambda_a, \zeta_a^n) = 2\int_0^\infty \mathrm{d}x \, \frac{x\mathrm{J}_n^2(x\sqrt{2\lambda_a})}{(1 + x^2/\kappa_a)^{\kappa_a + 3/2}} Q_a^n(x), \tag{3.28}$$

with the following functions:

$$H_a^n(x) = -\left(1 - \frac{1}{4\kappa_a^2}\right) A_a + \frac{(\xi_a - A_a \zeta_a^n)}{\sqrt{1 + x^2/\kappa_a}} Z_\kappa^{(1,2)}\left(\frac{\zeta_a^n}{\sqrt{1 + x^2/\kappa_a}}\right), \tag{3.29}$$

https://doi.org/10.1017/S0022377821000593 Published online by Cambridge University Press

$$\mathrm{K}_a^n(x) = \left(1 - \frac{1}{4\kappa_a^2}\right)\xi_a + \left(\zeta_a^n + \frac{U_a}{\alpha_{\parallel a}}\right) H_a^n(x), \tag{3.30}$$

$$Q_a^n(x) = \xi_a \left(1 - \frac{1}{4\kappa_a^2}\right)\left(\zeta_a^n + \frac{2U_a}{\alpha_{\parallel a}}\right) + \left(\zeta_a^n + \frac{U_a}{\alpha_{\parallel a}}\right)^2 H_a^n(x). \tag{3.31}$$

In this way, we only need to implement the modified plasma dispersion function $Z_\kappa^{(1,2)}$. This function can be directly evaluated using (B7) for integer values of κ, or (B1) for real values of κ. Integrals in (3.23)–(3.28) are evaluated using an adaptive numerical quadrature based in the routine QUADPACK (Piessens *et al.* 1983).

3.1. *Maxwellian limit*

In the limit $\kappa_a \to \infty$ we recover the dispersion tensor for a drifting bi-Maxwellian plasma (Stix 1992), by using the following limits:

$$\lim_{\kappa_a\to\infty} \mathrm{Z}_{n,k}^{(\alpha,\beta)}(\lambda_a, \zeta_a^n) = \Lambda_n(\lambda_a) Z(\zeta_a^n), \tag{3.32}$$

$$\lim_{\kappa_a\to\infty} \mathrm{Y}_{n,k}^{(\alpha,\beta)}(\lambda_a, \zeta_a^n) = \Lambda_n'(\lambda_a) Z(\zeta_a^n), \tag{3.33}$$

$$\lim_{\kappa_a\to\infty} \left(1 + y^2/\kappa_a\right)^{-(\kappa+\alpha)} = \mathrm{e}^{-y^2}. \tag{3.34}$$

Here $\Lambda_n(x) = \mathrm{I}_n(x)\mathrm{e}^{-x}$, with $\mathrm{I}_n(x)$ the modified Bessel function, and $Z(x)$ is the plasma dispersion function for Maxwellian distributed plasmas (Fried & Conte 1961). Thus, the elements of the dispersion tensor reduce to

$$D_{11} = 1 - \frac{c^2k_\parallel^2}{\omega^2} + \sum_a \frac{\omega_{\mathrm{pa}}^2}{\omega^2} \sum_{n=-\infty}^{\infty} \frac{n^2}{\lambda_a} \Lambda_n(\lambda_a) \mathcal{A}_n, \tag{3.35}$$

$$D_{22} = 1 - \frac{c^2k^2}{\omega^2} + \sum_a \frac{\omega_{\mathrm{pa}}^2}{\omega^2} \sum_{n=-\infty}^{\infty} \left(\frac{n^2}{\lambda_a}\Lambda_n(\lambda_a) - 2\lambda_a \Lambda_n'(\lambda_a)\right) \mathcal{A}_n, \tag{3.36}$$

$$D_{12} = \sum_a \frac{\omega_{\mathrm{pa}}^2}{\omega^2} \sum_{n=-\infty}^{\infty} n\Lambda_n(\lambda_a) \mathcal{A}_n, \tag{3.37}$$

$$D_{13} = \frac{c^2k_\perp k_\parallel}{\omega^2} + 2\sum_a \frac{q_a}{|q_a|}\frac{\omega_{\mathrm{pa}}^2}{\omega^2}\sqrt{\frac{T_{\parallel a}}{T_{\perp a}}} \sum_{n=-\infty}^{\infty} \frac{n}{\sqrt{2\lambda_a}} \Lambda_n(\lambda_a)\mathcal{B}_n, \tag{3.38}$$

$$D_{23} = -2\sum_a \frac{\omega_{\mathrm{pa}}^2}{\omega^2}\frac{|q_a|}{q_a}\sqrt{\frac{T_{\parallel a}}{T_{\perp a}}}\sqrt{\frac{\lambda_a}{2}} \sum_{n=-\infty}^{\infty} \Lambda_n'(\lambda_a)\mathcal{B}_n, \tag{3.39}$$

$$D_{33} = 1 - \frac{c^2k_\perp^2}{\omega^2} + 2\sum_a \frac{\omega_{\mathrm{pa}}^2}{\omega^2}\frac{T_{\parallel a}}{T_{\perp a}}\frac{U_a}{\alpha_{\parallel a}}\left(\frac{U_a}{\alpha_{\parallel a}} + 2\xi_a\right) + 2\sum_a \frac{\omega_{\mathrm{pa}}^2}{\omega^2}\frac{T_{\parallel a}}{T_{\perp a}} \sum_{n=-\infty}^{\infty} \Lambda_n(\lambda_a)\mathcal{C}_n, \tag{3.40}$$

$$\mathcal{A}_n = -A_a + (\xi_a - A_a\zeta_a^n) Z(\zeta_a^n), \tag{3.41}$$

$$\mathcal{B}_n = \xi_a + \left(\zeta_a^n + \frac{U_a}{\alpha_{\parallel a}}\right)\mathcal{A}_n, \tag{3.42}$$

https://doi.org/10.1017/S0022377821000593 Published online by Cambridge University Press

$$\mathcal{C}_n = \xi_a \zeta_a^n + \left(\zeta_a^n + \frac{U_a}{\alpha_{\parallel a}}\right)^2 \mathcal{A}_n. \tag{3.43}$$

These expressions are equivalent to those provided in Stix (1992, pp. 258–260).

3.2. *Non-drifting bi-Kappa*

For components (3.2)–(3.7) of the dielectric tensor, in the non-drifting limit $U_a = 0$ we recover the results for bi-Kappa plasmas (Gaelzer *et al.* 2016; Kim *et al.* 2017),

$$D_{11} = 1 - \frac{c^2 k_\parallel^2}{\omega^2} + \sum_a \frac{\omega_{\mathrm{pa}}^2}{\omega^2} \sum_{n=-\infty}^{\infty} \frac{n^2}{\lambda_a} \left[\xi_a Z_{n,\kappa}^{(1,2)}(\lambda_a, \zeta_a^n) + \frac{A_a}{2} \frac{\partial}{\partial \zeta_a^n} Z_{n,k}^{(1,1)}(\lambda_a, \zeta_a^n) \right], \tag{3.44}$$

$$D_{22} = 1 - \frac{c^2 k^2}{\omega^2} + \sum_a \frac{\omega_{\mathrm{pa}}^2}{\omega^2} \sum_{n=-\infty}^{\infty} \left[\xi_a W_{n,\kappa}^{(1,2)}(\lambda_a, \zeta_a^n) + \frac{A_a}{2} \frac{\partial}{\partial \zeta_a^n} W_{n,k}^{(1,1)}(\lambda_a, \zeta_a^n) \right], \tag{3.45}$$

$$D_{12} = \sum_a \frac{\omega_{\mathrm{pa}}^2}{\omega^2} \sum_{n=-\infty}^{\infty} n \left[\xi_a \frac{\partial}{\partial \lambda_a} Z_{n,\kappa}^{(1,2)}(\lambda_a, \zeta_a^n) + \frac{A_a}{2} \frac{\partial^2}{\partial \lambda_a \partial \zeta_a^n} Z_{n,k}^{(1,1)}(\lambda_a, \zeta_a^n) \right], \tag{3.46}$$

$$D_{13} = \frac{c^2 k_\perp k_\parallel}{\omega^2} - \sum_a \frac{q_a}{|q_a|} \frac{\omega_{\mathrm{pa}}^2}{\omega^2} \sqrt{\frac{T_{\parallel a}}{T_{\perp a}}} \sum_{n=-\infty}^{\infty} \frac{n}{\sqrt{2\lambda_a}} \left(\xi_a - A_a \zeta_a^n\right) \frac{\partial}{\partial \zeta_a^n} Z_{n,\kappa}^{(1,1)}(\lambda_a, \zeta_a^n), \tag{3.47}$$

$$D_{23} = \sum_a \frac{\omega_{\mathrm{pa}}^2}{\omega^2} \frac{|q_a|}{q_a} \sqrt{\frac{T_{\parallel a}}{T_{\perp a}}} \sqrt{\frac{\lambda_a}{2}} \sum_{n=-\infty}^{\infty} \left(\xi_a - A_a \zeta_a^n\right) \frac{\partial^2}{\partial \lambda_a \partial \zeta_a^n} Z_{n,\kappa}^{(1,1)}(\lambda_a, \zeta_a^n), \tag{3.48}$$

$$D_{33} = 1 - \frac{c^2 k_\perp^2}{\omega^2} - \sum_a \frac{\omega_{\mathrm{pa}}^2}{\omega^2} \frac{T_{\parallel a}}{T_{\perp a}} \sum_{n=-\infty}^{\infty} \zeta_a^n (\xi_a - A_a \zeta_a^n) \frac{\partial}{\partial \zeta_a^n} Z_{n,\kappa}^{(1,1)}(\lambda_a, \zeta_a^n). \tag{3.49}$$

4. Numerical results

In this section we present the results obtained with our new solver DIS-K, which implements the new dispersion tensor for plasmas with drifting bi-Kappa distributions. This solver can also be used for any of the bi-Maxwellian or non-drifting limits discussed above.

Here we show a number of illustrative examples of stable and unstable solutions obtained with the new solver DIS-K. As this is the first reported solver for drifting bi-Kappa plasmas, for its testing we can choose only from the limit configurations discussed above, and which can also be resolved by other solvers. As we know, DHSARK (Astfalk *et al.* 2015) is programmed to derive the unstable electromagnetic solutions of anisotropic plasma populations described by bi-Kappa distributions (Astfalk 2018). We will use the aperiodic electron firehose instability, as described in Shaaban *et al.* (2019) and López *et al.* (2019), as a first test case. We consider an anisotropic electron distribution with $T_{\perp e}/T_{\parallel e} = 0.5$, and with $\beta_{\parallel e} = 8\pi n_e T_{\parallel e}/B_0^2 = 4.0$, $\omega_{\mathrm{pe}}/\Omega_e = 100$, $\theta = 50^\circ$, $\kappa_e = 4$, and protons are modelled using an isotropic Maxwellian distribution with $\beta_p = 4.0$. Figure 1 displays the unstable solutions obtained solving the set of equations presented in § 3.2. Panel (*a*) shows the real part of the normalized frequency, ω_r/Ω_e versus the normalized wave number ck/ω_{pe}. As expected from the aperiodic nature of this instability, the wave frequency is zero for the entire range of unstable modes. Panel (*b*) of this figure shows the growth rate, γ/Ω_e versus ck/ω_{pe}, which coincides with that obtained using DSHARK in Shaaban *et al.* (2019), plotted here with red dots. The solutions of both codes

https://doi.org/10.1017/S0022377821000593 Published online by Cambridge University Press

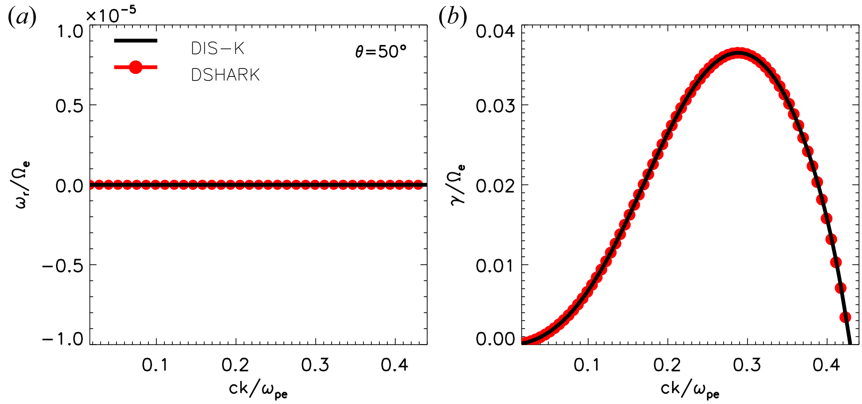

FIGURE 1. Unstable solutions of the aperiodic electron firehose instability at $\theta = 50^\circ$. In black are the solutions obtained with the new code, DIS-K, while red dots are obtained with DSHARK. Panel (*a*) shows the normalized (real) frequency, ω_r/Ω_e versus the normalized wavenumber ck/ω_{pe}, and panel (*b*) shows the normalized growth rate, γ/Ω_e versus ck/ω_{pe}.

show a perfect match for this case, validating our new solver DIS-K in the non-drifting bi-Kappa limit, $U_a = 0$, discussed in § 3.2.

We now discuss damped solutions in order to test the analytical continuation of our modified plasma dispersion function. Expression in (B1) for arbitrary κ or (B7) for integer κ, already satisfy the Landau prescription, being analytically continuous through the entire complex frequency plane (Summers & Thorne 1991; Mace & Hellberg 1995; Gaelzer & Ziebell 2016). In this case we study a damped kinetic Alfvén wave (KAW) propagating at highly oblique angles, $\theta = 88^\circ$. We use $\beta_e = \beta_p = 2.0$, $v_A/c = 2.33 \times 10^{-4}$ (or $\omega_{\text{pe}}/\Omega_{\text{ce}} = 100$), where $v_A = B_0/\sqrt{4\pi n_p m_p}$ is the Alfvén speed. In figure 2 we compare our results with those obtained with another solver, NHDS (Verscharen & Chandran 2018) providing solutions in the Maxwellian limit. Blue dots correspond to the solution obtained with NHDS, while the black line is our solution in the Maxwellian limit, $\kappa_p = \infty$. We have also included solutions for $\kappa_p = 10$ (green dot–dashed lines) and $\kappa_p = 2$ (red dotted lines), to show the behaviour of our code in the Kappa regime. In the Maxwellian limit both codes show a perfect agreement. For finite but large values of κ_p the solution is similar to the Maxwellian case, but differences start appearing at large wavenumbers. Overall, suprathermal particles reduce the damping of KAWs at large wavenumbers (Kim *et al.* 2018).

In the following, we test the drifting case. Now, DSHARK is not programmed to solve the dispersion relation for drifting bi-Kappa distributions, and the NHDS solver is only foreseen to operate with drifting bi-Maxwellian distributions, as described in § 3.1. Therefore, we have to settle for this limiting case. For this comparison we choose conditions for the oblique whistler heat-flux instability, as described in López *et al.* (2020). We consider a plasma composed of two electron populations, a dense central core (subscript c) and a tenuous suprathermal beam (subscript b), with a relative drift along the background magnetic field, with the following properties: $n_c/n_0 = 0.95$, $n_b/n_0 = 0.05$ are the core and beam normalized number density, respectively, $T_{\parallel b}/T_{\parallel c} = 4.0$, $T_{\perp j}/T_{\parallel j} = 1.0$, $\omega_{\text{pe}}/\Omega_e = 100$, $\beta_c = 8\pi n_0 T_c/B_0^2 = 2.0$ and $U_b/c = 0.035$ (or $U_b/v_A = 150$). Figure 3 shows the dispersion relation obtained for $\theta = 60^\circ$. This time we plot the solution obtained using the NHDS solver as a blue dots. In the range of wavenumbers resolved we show both

https://doi.org/10.1017/S0022377821000593 Published online by Cambridge University Press

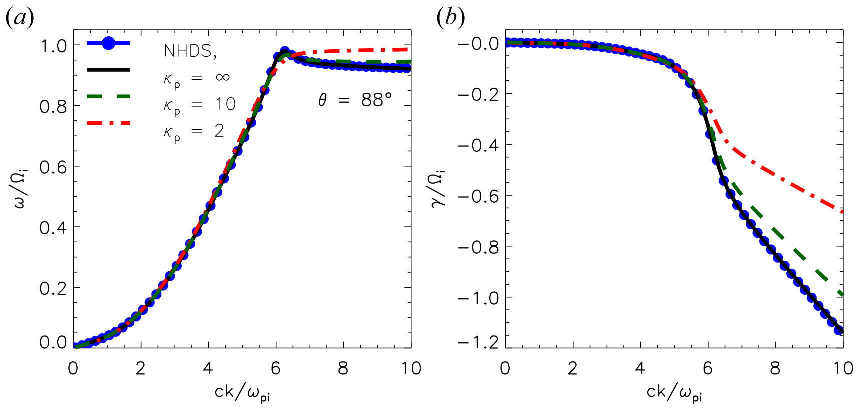

FIGURE 2. The damped KAW solutions at $\theta = 88^\circ$: blue dots are obtained with NHDS; those obtained with the present code, DIS-K, are black lines for $\kappa_p = \infty$ (Maxwellian limit); green dot–dashed line for $\kappa_p = 10$; red dotted line for $\kappa_p = 2$. Panel (*a*) shows ω_r/Ω_i versus $ck/\omega_{\rm pi}$ and panel (*b*) γ/Ω_i versus $ck/\omega_{\rm pi}$.

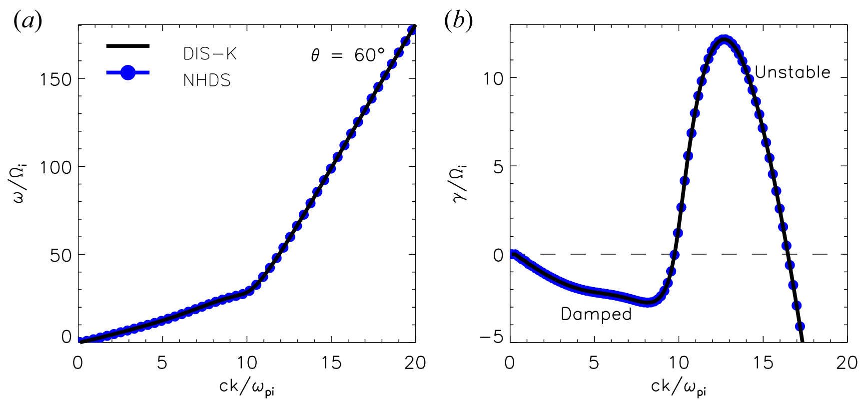

FIGURE 3. The oblique whistler heat-flux instability at $\theta = 60^\circ$: black lines are solutions obtained with the present code, DIS-K; blue dots correspond to NHDS. Panel (*a*) shows ω_r/Ω_i versus $ck/\omega_{\rm pi}$ and panel (*b*) γ/Ω_i versus $ck/\omega_{\rm pi}$.

damped and unstable modes. We can clearly observe the agreement between both codes, in the real and imaginary parts of the frequency, for damped and unstable modes.

Finally, assuming the same plasma conditions, we explore the same instability under the influence of suprathermal electrons, showing the results obtained with DIS-K for drifting bi-Kappa electrons. Figure 4 shows, comparatively, three different cases. For comparison, panel (*a*) shows the solution for drifting Maxwellian electrons, as in figure 3, but this time for the entire range of angles of propagation. Panel (*b*) displays a new case, when core electrons are modelled by a Kappa distribution with $\kappa_c = 2$, while the beam remains Maxwellian ($\kappa_b = \infty$). Panel (*c*) shows the case when both, core and beam populations are modelled by a Kappa distribution with the same kappa index, $\kappa_c = \kappa_b = 2$. We observe that suprathermal electrons suppress the oblique whistler heat-flux instability. When the core is Kappa distributed, the range of unstable angles and wavenumbers is reduced, as well as the level of the unstable modes. The suppressing effect is even more prominent

https://doi.org/10.1017/S0022377821000593 Published online by Cambridge University Press

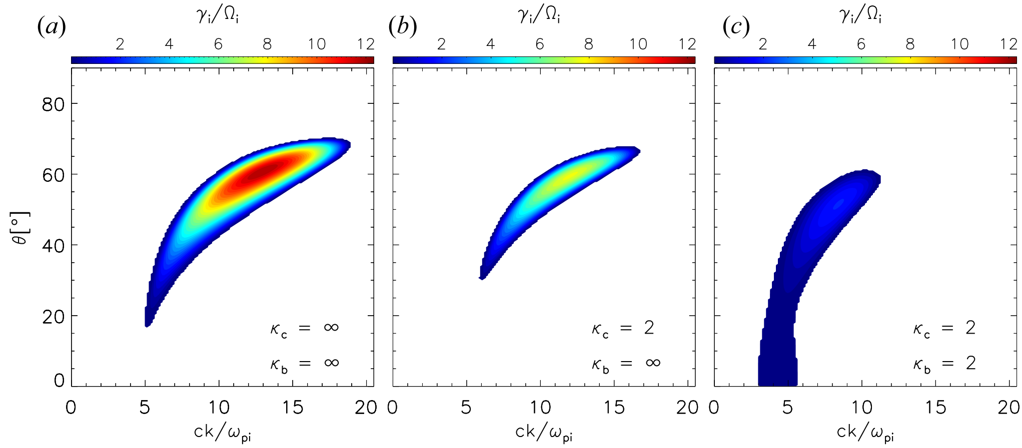

FIGURE 4. The oblique whistler heat-flux growth rates for all angles of propagation, and for various core-beam configurations described in the text.

when both populations are Kappa distributed, reaching lower growth rates and shifting to lower angles. We can identify some possible explanations of these inhibiting effects, either in the core damping, which counteracts the strahl-driving of the oblique whistler instability, but also by a change in resonance conditions (populations involved, etc.), in this case, implying both Landau and cyclotron resonances. On the other hand, the enhanced suprathermal tails reduce the effective excess of free energy in parallel (drifting) direction (with increasing the tails the core and beam electrons tend to merge and combine with each other, reducing the relative drift between them). Indeed, in the last case, we also obtain unstable modes in parallel and quasi-parallel (low angles) directions, specific to lower drifts.

5. Conclusions

We have presented the full set of components of the dielectric tensor for magnetized plasma populations modelled by drifting bi-Kappa distributions. This extended dielectric tensor has been implemented in a new dispersion solver, named DIS-K, and capable of resolving the full spectrum of stable and unstable modes of these complex plasma distributions. In order to validate our results and our code, we carried out illustrative cases enabling comparison with limiting conditions, e.g. non-drifting bi-Kappa and drifting bi-Maxwellian plasmas, resolved by the existing solvers. For comparison, the the aperiodic electron firehose solutions driven by (non-drifting) bi-Kappa electrons are obtained with DSHARK, and we found a perfect agreement for both the wavenumber dispersion of the wave frequency and growth rate. The same remarkable agreement has been obtained with the stable and unstable whistler-like modes triggered by drifting bi-Maxwellian electrons populations and described by another solver, NHDS. We have also shown the capabilities of our code to handle damped solutions, as shown for the KAW dispersion curves, showing a perfect agreement when compared with NHDS in the Maxwellian limit. Further, we have explored the influence of suprathermal electrons on the oblique whistler heat-flux instability, showing that the instability is inhibited, i.e. growth rates are diminished (and the range of unstable wavenumbers is reduced), when core and beam electrons are modelled by drifting bi-Kappa distributions. We plan make this new code, DIS-K, publicly available in the near future.

https://doi.org/10.1017/S0022377821000593 Published online by Cambridge University Press

These are new theoretical and numerical tools, which extend and improve the existing capabilities of analysis of the wave fluctuations, stable or unstable modes, specific to the complex particles configurations unveiled by the in-situ observations in space plasmas. Thus, applications can be considered in the context of solar wind and planetary environments, where all plasma species (electrons and ions) exhibit multiple drifting components, namely, core, halo and strahl, populated by suprathermals and with intrinsic anisotropies (i.e. anisotropic temperatures).

Acknowledgements

We thank J.A. Araneda for his valuable contribution to the development of this code. We also thank the anonymous reviewers for their insightful comments.

Editor Thierry Passot thanks the referees for their advice in evaluating this article.

Funding

R.A.L. acknowledges the support of ANID Chile through FONDECyT grant no. 11201048. We also acknowledge the support of the projects SCHL 201/35-1 (DFG-German Research Foundation), C14/ 19/089 (C1 project Internal Funds KU Leuven), G.0A23.16N (FWO-Vlaanderen) and C 90347 (ESA Prodex). S.M. Shaaban acknowledges the Alexander-von-Humboldt Research Fellowship, Germany.

Declaration of interests

The authors report no conflict of interest.

Appendix A. Summary of necessary functions

$$Z_{n,\kappa}^{(1,2)}(\lambda_a,\zeta_a^n)=2\int_0^\infty \mathrm{d}x\,\frac{x\mathrm{J}_n^2(x\sqrt{2\lambda_a})}{(1+x^2/\kappa)^{\kappa+2}}Z_\kappa^{(1,2)}\left(\frac{\zeta_a^n}{\sqrt{1+x^2/\kappa}}\right), \tag{A1}$$

$$\frac{\partial}{\partial\zeta_a^n}Z_{n,k}^{(1,1)}(\lambda_a,\zeta_a^n)=2\int_0^\infty \mathrm{d}x\,\frac{x\mathrm{J}_n^2(x\sqrt{2\lambda_a})}{(1+x^2/\kappa)^{\kappa+3/2}}Z'^{(1,1)}_\kappa\left(\frac{\zeta_a^n}{\sqrt{1+x^2/\kappa}}\right), \tag{A2}$$

$$\mathrm{Y}_{n,\kappa}^{(1,2)}(\lambda_a,\zeta_a^n)=\frac{2}{\lambda_a}\int_0^\infty \mathrm{d}x\,\frac{x^3\mathrm{J}_{n-1}(x\sqrt{2\lambda_a})\mathrm{J}_{n+1}(x\sqrt{2\lambda_a})}{(1+x^2/\kappa)^{\kappa+2}}Z_\kappa^{(1,2)}\left(\frac{\zeta_a^n}{\sqrt{1+x^2/\kappa}}\right), \tag{A3}$$

$$W_{n,\kappa}^{(1,2)}(\lambda_a,\zeta_a^n)=\frac{n^2}{\lambda_a}Z_{n,\kappa}^{(1,2)}(\lambda_a,\zeta_a^n)-2\lambda_a\mathrm{Y}_{n,\kappa}^{(1,2)}(\lambda_a,\zeta_a^n), \tag{A4}$$

$$\frac{\partial}{\partial\zeta_a^n}\mathrm{Y}_{n,k}^{(1,1)}(\lambda_a,\zeta_a^n)=\frac{2}{\lambda_a}\int_0^\infty \mathrm{d}x\,\frac{x^3\mathrm{J}_{n-1}(x\sqrt{2\lambda_a})\mathrm{J}_{n+1}(x\sqrt{2\lambda_a})}{(1+x^2/\kappa_a)^{\kappa_a+3/2}}Z'^{(1,1)}_\kappa\left(\frac{\zeta_a^n}{\sqrt{1+x^2/\kappa}}\right), \tag{A5}$$

$$\frac{\partial}{\partial\zeta_a^n}W_{n,k}^{(1,1)}(\lambda_a,\zeta_a^n)=\frac{n^2}{\lambda_a}\frac{\partial}{\partial\zeta_a^n}Z_{n,\kappa}^{(1,1)}(\lambda_a,\zeta_a^n)-2\lambda_a\frac{\partial}{\partial\zeta_a^n}\mathrm{Y}_{n,\kappa}^{(1,1)}(\lambda_a,\zeta_a^n), \tag{A6}$$

$$\begin{aligned}\frac{\partial}{\partial\lambda_a}Z_{n,\kappa}^{(1,2)}(\lambda,\zeta_a^n)=\frac{2}{\sqrt{2\lambda_a}}\int_0^\infty \mathrm{d}x\,&\frac{x^2\mathrm{J}_n(x\sqrt{2\lambda_a})[\mathrm{J}_{n-1}(x\sqrt{2\lambda_a})-\mathrm{J}_{n+1}(x\sqrt{2\lambda_a})]}{(1+x^2/\kappa)^{\kappa+2}}\\&\times Z_\kappa^{(1,2)}\left(\frac{\zeta_a^n}{\sqrt{1+x^2/\kappa}}\right),\end{aligned} \tag{A7}$$

https://doi.org/10.1017/S0022377821000593 Published online by Cambridge University Press

$$\frac{\partial^2}{\partial\lambda\partial\zeta_a^n}Z_{n,k}^{(1,1)}(\lambda_a,\zeta_a^n)=\frac{2}{\sqrt{2\lambda_a}}\int_0^\infty \mathrm{d}x\,\frac{x^2\mathrm{J}_n(x\sqrt{2\lambda_a})[\mathrm{J}_{n-1}(x\sqrt{2\lambda_a})-\mathrm{J}_{n+1}(x\sqrt{2\lambda_a})]}{(1+x^2/\kappa)^{\kappa+3/2}}\times Z_\kappa'^{(1,1)}\left(\frac{\zeta_a^n}{\sqrt{1+x^2/\kappa}}\right). \tag{A8}$$

Appendix B. Some useful functions

The modified $Z_\kappa^{(\alpha,\beta)}$ function can be calculated in terms of the hypergeometric function as (Gaelzer & Ziebell 2016)

$$Z_\kappa^{(\alpha,\beta)}(\zeta_a^n)=\frac{\mathrm{i}}{\kappa^{\beta+1}}\frac{\Gamma(\kappa+\alpha+\beta-1)\Gamma(\kappa+\alpha+\beta-1/2)}{\Gamma(\kappa)\Gamma(\kappa+\alpha-3/2)}\times\,{}_2F_1\left[1,2(\kappa+\alpha+\beta-1);\lambda;\left(\frac{\mathrm{i}\sqrt{\kappa}-\zeta_a^n}{2\mathrm{i}\sqrt{\kappa}}\right)\right]. \tag{B1}$$

Then, using

$$\frac{\mathrm{d}}{\mathrm{d}z}\,{}_2F_1[a,b;c;z]=\frac{ab}{c}\,{}_2F_1[a+1,b+1;c+1;z], \tag{B2}$$

we have

$$\frac{\partial}{\partial\zeta_a^n}Z_\kappa^{(\alpha,\beta)}(\zeta_a^n)=-\frac{1}{\kappa^{\beta+1}}\frac{\Gamma(\kappa+\alpha+\beta)\Gamma(\kappa+\alpha+\beta-1/2)}{\Gamma(\kappa+\alpha+\beta+1)\Gamma(\kappa+\alpha-3/2)}\times\,{}_2F_1\left[2,2(\kappa+\alpha+\beta-1)+1;\kappa+\alpha+\beta+1;\left(\frac{\mathrm{i}\sqrt{\kappa}-\zeta_a^n}{2i\sqrt{\kappa}}\right)\right]. \tag{B3}$$

Also, a useful expression is obtained from Gaelzer & Ziebell (2016):

$$Z_\kappa'^{(\alpha,\beta)}(\zeta_a^n)=-2\left[\frac{\Gamma(\kappa+\alpha+\beta-1/2)}{\kappa^{\beta+1}\Gamma(\kappa+\alpha-3/2)}+\zeta_a^nZ_\kappa^{(\alpha,\beta+1)}(\zeta_a^n)\right]. \tag{B4}$$

We can obtain a simpler expression if κ is assumed integer, as in Summers & Thorne (1991). Then we have

$$Z_\kappa^{(\alpha,\beta)}(\xi)=\frac{\mathrm{i}}{2^{2(1-\lambda)}\kappa^{\beta+1/2}}\frac{\Gamma(\lambda-1)^2\Gamma(\lambda-1/2)}{\Gamma(\kappa+\alpha-3/2)\Gamma[2(\lambda-1)]}\left(\frac{\kappa+\xi^2}{\kappa}\right)^{1-\lambda}\times\left\{1-\left(\frac{\mathrm{i}\sqrt{\kappa}+\xi}{2i\sqrt{\kappa}}\right)^{\lambda-1}\frac{1}{\Gamma(\lambda-1)}\sum_{\ell=0}^{\lambda-2}\frac{\Gamma[\ell+\lambda-1]}{\Gamma(\ell+1)}\left(\frac{\mathrm{i}\sqrt{\kappa}-\xi}{2\mathrm{i}\sqrt{\kappa}}\right)^\ell\right\}. \tag{B5}$$

Let us take a look to some particular values:

$$Z_\kappa^{(1,1)}(\xi)=\frac{2\mathrm{i}\pi^{1/2}}{\kappa^{3/2}}\frac{\kappa!}{\Gamma(\kappa-1/2)}\left(\frac{\kappa+\xi^2}{\kappa}\right)^{-\kappa-1}\left\{1-\frac{1}{\kappa!}\left(\frac{\mathrm{i}\sqrt{\kappa}+\xi}{2\mathrm{i}\sqrt{\kappa}}\right)^{\kappa+1}\sum_{\ell=0}^{\kappa}\frac{(\ell+\kappa)!}{\ell!}\left(\frac{i\sqrt{\kappa}-\xi}{2i\sqrt{\kappa}}\right)^\ell\right\}. \tag{B6}$$

https://doi.org/10.1017/S0022377821000593 Published online by Cambridge University Press

Also, we are also interested in

$$Z_\kappa^{(1,2)}(\xi) = \frac{2\mathrm{i}\pi^{1/2}}{\kappa^{5/2}} \frac{(\kappa+1)!}{\Gamma(\kappa-1/2)} \left(\frac{\kappa+\xi^2}{\kappa}\right)^{-\kappa-2} \left\{1 - \frac{1}{(\kappa+1)!}\left(\frac{\mathrm{i}\sqrt{\kappa}+\xi}{2\mathrm{i}\sqrt{\kappa}}\right)^{\kappa+2} \sum_{\ell=0}^{\kappa+1} \frac{(\ell+\kappa+1)!}{\ell!}\left(\frac{\mathrm{i}\sqrt{\kappa}-\xi}{2i\sqrt{\kappa}}\right)^{\ell}\right\}. \tag{B7}$$

For the derivative, we have

$$Z'^{(1,1)}_\kappa(\zeta_a^n) = -\frac{\mathrm{i}\zeta_a^n}{\kappa^{5/2}} \frac{\Gamma(\kappa+2)^2\Gamma(\kappa+3/2)}{\Gamma(\kappa-1/2)\Gamma(2\kappa+3)} \left(\frac{\kappa+(\zeta_a^n)^2}{4\kappa}\right)^{-\kappa-2} \left\{1 - \frac{\sqrt{\kappa}}{\mathrm{i}\zeta_a^n}\left(\frac{\mathrm{i}\sqrt{\kappa}+\zeta_a^n}{2\mathrm{i}\sqrt{\kappa}}\right)^{\kappa+2} \times \frac{1}{\Gamma(\kappa+2)} \sum_{\ell=0}^{\kappa+1} \frac{\Gamma(\ell+\kappa+1)}{\Gamma(\ell+1)}(\ell-\kappa-1)\left(\frac{\mathrm{i}\sqrt{\kappa}-\zeta_a^n}{2\mathrm{i}\sqrt{\kappa}}\right)^{\ell}\right\}. \tag{B8}$$

REFERENCES

ALEXANDROVA, O., CHEN, C.H.K., SORRISO-VALVO, L., HORBURY, T.S. & BALE, S.D. 2013 Solar wind turbulence and the role of ion instabilities. *Space Sci. Rev*. **178** (2), 101–139.

ASTFALK, P. 2018 Linear and quasilinear studies of kinetic instabilities in non-Maxwellian space plasmas. Dissertation, Technische Universität, München, München.

ASTFALK, P., GÖRLER, T. & JENKO, F. 2015 DSHARK: a dispersion relation solver for obliquely propagating waves in bi-kappa-distributed plasmas. *J. Geophys. Res.: Space* **120** (9), 7107–7120.

BALE, S.D., KASPER, J.C., HOWES, G.G., QUATAERT, E., SALEM, C. & SUNDKVIST, D. 2009 Magnetic fluctuation power near proton temperature anisotropy instability thresholds in the solar wind. *Phys. Rev. Lett*. **103**, 211101.

BASU, B. 2009 Hydromagnetic waves and instabilities in kappa distribution plasma. *Phys. Plasmas* **16** (5), 052106.

BIAN, N.H., EMSLIE, A.G., STACKHOUSE, D.J. & KONTAR, E.P. 2014 The formation of Kappa-distribution accelerated electron populations in solar flares. *Astrophys. J*. **796** (2), 142.

BOWEN, T.A., MALLET, A., HUANG, J., KLEIN, K.G., MALASPINA, D.M., STEVENS, M., BALE, S.D., BONNELL, J.W., CASE, A.W., CHANDRAN, B.D.G., *et al.* 2020 Ion-scale electromagnetic waves in the inner heliosphere. *Astrophys. J. Suppl*. **246** (2), 66.

CATTAERT, T., HELLBERG, M.A. & MACE, R.L. 2007 Oblique propagation of electromagnetic waves in a kappa-Maxwellian plasma. *Phys. Plasmas* **14** (8), 082111.

COLLIER, M.R., HAMILTON, D., GLOECKLER, G., BOCHSLER, P. & SHELDON, R. 1996 Neon-20, oxygen-16, and helium-4 densities, temperatures, and suprathermal tails in the solar wind determined with wind/mass. *Geophys. Res. Lett*. **23** (10), 1191–1194.

FRIED, B. & CONTE, S. 1961 *The Plasma Dispersion Function: The Hilbert Transform of the Gaussian*. Academic Press.

GAELZER, R. & ZIEBELL, L.F. 2016 Obliquely propagating electromagnetic waves in magnetized kappa plasmas. *Phys. Plasmas* **23** (2), 022110.

GAELZER, R., ZIEBELL, L.F. & MENESES, A.R. 2016 The general dielectric tensor for bi-kappa magnetized plasmas. *Phys. Plasmas* **23** (6), 062108.

GARY, S.P. 1993 *Theory of Space Plasma Microinstabilities*. Cambridge University Press.

GARY, S.P., JIAN, L.K., BROILES, T.W., STEVENS, M.L., PODESTA, J.J. & KASPER, J.C. 2016 Ion-driven instabilities in the solar wind: wind observations of 19 March 2005. *J. Geophys. Res.: Space* **121**, 30–41.

HAMMOND, C.M., FELDMAN, W.C., MCCOMAS, D.J., PHILLIPS, J.L. & FORSYTH, R.J. 1996 Variation of electron-strahl width in the high-speed solar wind: ULYSSES observations. *Astron. Astrophys*. **316**, 350–354.

https://doi.org/10.1017/S0022377821000593 Published online by Cambridge University Press

HELLBERG, M.A. & MACE, R.L. 2002 Generalized plasma dispersion function for a plasma with a kappa-Maxwellian velocity distribution. *Phys. Plasmas* **9** (5), 1495.

ISENBERG, P.A. & VASQUEZ, B.J. 2019 Perpendicular ion heating by cyclotron resonant dissipation of turbulently generated kinetic Alfvén waves in the solar wind. *Astrophys. J.* **887** (1), 63.

JEONG, S.-Y., VERSCHAREN, D., WICKS, R.T. & FAZAKERLEY, A.N. 2020 A quasi-linear diffusion model for resonant wave-particle instability in homogeneous plasma. *Astrophys. J.* **902** (2), 128.

KASPER, J.C., LAZARUS, A.J., GARY, S.P. & SZABO, A. 2003 Solar wind temperature anisotropies. *AIP Conf. Proc*. **679** (1), 538–541.

KIM, S., LAZAR, M., SCHLICKEISER, R., LÓPEZ, R.A. & YOON, P.H. 2018 Low frequency electromagnetic fluctuations in Kappa magnetized plasmas. *Plasma Phys. Control. Fusion* **60** (7), 075010.

KIM, S., SCHLICKEISER, R., YOON, P.H., LÓPEZ, R.A. & LAZAR, M. 2017 Spontaneous emission of electromagnetic fluctuations in Kappa magnetized plasmas. *Plasma Phys. Control. Fusion* **59** (12), 125003.

KLEIN, K.G. & HOWES, G.G. 2015 Predicted impacts of proton temperature anisotropy on solar wind turbulence. *Phys. Plasmas* **22** (3), 032903.

LAZAR, M., FICHTNER, H. & YOON, P.H. 2016 On the interpretation and applicability of κ-distributions. *Astron. Astrophys*. **589**, A39.

LAZAR, M., LÓPEZ, R.A., SHAABAN, S.M., POEDTS, S. & FICHTNER, H. 2019 Whistler instability stimulated by the suprathermal electrons present in space plasmas. *Astrophys. Space Sci*. **364** (10), 171.

LAZAR, M., PIERRARD, V., SHAABAN, S., FICHTNER, H. & POEDTS, S. 2017 Dual Maxwellian-kappa modeling of the solar wind electrons: new clues on the temperature of kappa populations. *Astron. Astrophys*. **602**, A44.

LAZAR, M. & POEDTS, S. 2009 Firehose instability in space plasmas with bi-kappa distributions. *Astron. Astrophys*. **494** (1), 311–315.

LAZAR, M., POEDTS, S. & FICHTNER, H. 2015 Destabilizing effects of the suprathermal populations in the solar wind. *Astron. Astrophys*. **582**, A124.

LAZAR, M., SCHERER, K., FICHTNER, H. & PIERRARD, V. 2020*a* Toward a realistic macroscopic parametrization of space plasmas with regularized κ-distributions. *Astron. Astrophys*. **634**, A20.

LEAMON, R.J., SMITH, C.W., NESS, N.F. & WONG, H.K. 1999 Dissipation range dynamics: kinetic Alfvé waves and the importance of β_e. *J. Geophys. Res.: Space* **104** (A10), 22331–22344.

LIU, Y., LIU, S.Q., DAI, B. & XUE, T.L. 2014 Dispersion and damping rates of dispersive Alfvén wave in a nonextensive plasma. *Phys. Plasmas* **21** (3), 032125.

LÓPEZ, R.A., LAZAR, M., SHAABAN, S.M., POEDTS, S. & MOYA, P.S. 2020 Alternative high-plasma beta regimes of electron heat-flux instabilities in the solar wind. *Astrophys. J. Lett*. **900** (2), L25.

LÓPEZ, R.A., LAZAR, M., SHAABAN, S.M., POEDTS, S., YOON, P.H., VIÑAS, A.F. & MOYA, P.S. 2019 Particle-in-cell simulations of firehose instability driven by bi-kappa electrons. *Astrophys. J. Lett*. **873** (2), L20.

MACE, R.L. & HELLBERG, M.A. 1995 A dispersion function for plasmas containing superthermal particles. *Phys. Plasmas* **2** (6), 2098.

MAKSIMOVIC, M., ZOUGANELIS, I., CHAUFRAY, J.-Y., ISSAUTIER, K., SCIME, E., LITTLETON, J., MARSCH, E., MCCOMAS, D., SALEM, C., LIN, R., *et al.* 2005 Radial evolution of the electron distribution functions in the fast solar wind between 0.3 and 1.5 au. *J. Geophys. Res.: Space* **110** (A9), A09104.

MARSCH, E. 2006 Kinetic physics of the solar corona and solar wind. *Living Rev. Sol. Phys*. **3** (1), 1–100.

MASON, G.M. & GLOECKLER, G. 2012 Power law distributions of suprathermal ions in the quiet solar wind. *Space Sci. Rev*. **172** (1–4), 241–251.

MICERA, A., ZHUKOV, A.N., LÓPEZ, R.A., INNOCENTI, M.E., LAZAR, M., BOELLA, E. & LAPENTA, G. 2020 Particle-in-cell simulation of whistler heat-flux instabilities in the solar wind: heat-flux regulation and electron halo formation. *Astrophys. J. Lett*. **903** (1), L23.

PIERRARD, V. & LAZAR, M. 2010 Kappa distributions: theory and applications in space plasmas. *Sol. Phys*. **267** (1), 153–174.

PIESSENS, R., DE DONCKER-KAPENGA, E., UEBERHUBER, C.W. & KAHANER, D.K. 1983 *Quadpack: A Subroutine Package for Automatic Integration*. Computational Mathematics Series. Springer.

PILIPP, W.G., MIGGENRIEDER, H., MONTGOMERY, M.D., MÜHLHÄUSER, K.H., ROSENBAUER, H. & SCHWENN, R. 1987 Characteristics of electron velocity distribution functions in the solar wind derived from the Helios Plasma Experiment. *J. Geophys. Res.* **92** (A2), 1075.

ROENNMARK, K. 1982 Waves in homogeneous, anisotropic multicomponent plasmas (whamp). *Rep. No. 179*, ISSN: 0347-6406. Kiruna, Sweden: Kiruna Geophysical Institute.

SHAABAN, S., LAZAR, M., LÓPEZ, R. & WIMMER-SCHWEINGRUBER, R. 2021*a* On the interplay of solar wind proton and electron instabilities: linear and quasi-linear approaches. *Mon. Not. R. Astron Soc.* **503** (3), 3134.

SHAABAN, S., LAZAR, M., YOON, P. & POEDTS, S. 2019 Quasilinear approach of the cumulative whistler instability in fast solar wind: constraints of electron temperature anisotropy. *Astron. Astrophys.* **627**, A76.

SHAABAN, S.M. & LAZAR, M. 2020 Whistler instabilities from the interplay of electron anisotropies in space plasmas: a quasi-linear approach. *Mon. Not. R. Astron Soc.* **492** (3), 3529–3539.

SHAABAN, S.M., LAZAR, M., LÓPEZ, R.A., FICHTNER, H. & POEDTS, S. 2019 Firehose instabilities triggered by the solar wind suprathermal electrons. *Mon. Not. R. Astron. Soc.* **483** (4), 5642–5648.

SHAABAN, S.M., LAZAR, M., LÓPEZ, R.A. & POEDTS, S. 2020 Electromagnetic ion–ion instabilities in space plasmas: effects of suprathermal populations. *Astrophys. J.* **899** (1), 20.

SHAABAN, S.M., LAZAR, M. & POEDTS, S. 2018 Clarifying the solar wind heat flux instabilities. *Mon. Not. R. Astron Soc.* **480** (1), 310–319.

SHAABAN, S.M., LAZAR, M. & SCHLICKEISER, R. 2021*b* Electromagnetic ion cyclotron instability stimulated by the suprathermal ions in space plasmas: a quasi-linear approach. *Phys. Plasmas* **28** (2), 022103.

STIX, T.H. 1992 *Waves in Plasmas*. AIP-Press.

ŠTVERÁK, Š., TRÁVNIČEK, P., MAKSIMOVIC, M., MARSCH, E., FAZAKERLEY, A.N. & SCIME, E.E. 2008 Electron temperature anisotropy constraints in the solar wind. *J. Geophys. Res.: Space* **113**, A03103.

SUMMERS, D. & THORNE, R.M. 1991 The modified plasma dispersion function. *Phys. Fluids* B **3** (8), 1835.

SUMMERS, D., XUE, S. & THORNE, R.M. 1994 Calculation of the dielectric tensor for a generalized Lorentzian (kappa) distribution function. *Phys. Plasmas* **1** (6), 2012–2025.

TONG, Y., VASKO, I.Y., ARTEMYEV, A.V., BALE, S.D. & MOZER, F.S. 2019 Statistical study of whistler waves in the solar wind at 1 au. *Astrophys. J.* **878** (1), 41.

VASYLIUNAS, V.M. 1968 A survey of low-energy electrons in the evening sector of the magnetosphere with OGO 1 and OGO 3. *J. Geophys. Res.* **73** (9), 2839–2884.

VERSCHAREN, D. & CHANDRAN, B.D.G. 2018 NHDS: the new Hampshire dispersion relation solver. *Res. Notes AAS* **2** (2), 13.

VERSCHAREN, D., CHANDRAN, B.D.G., JEONG, S.-Y., SALEM, C.S., PULUPA, M.P. & BALE, S.D. 2019*b* Self-induced scattering of Strahl electrons in the solar wind. *Astrophys. J.* **886** (2), 136.

VERSCHAREN, D., KLEIN, K.G. & MARUCA, B.A. 2019*a* The multi-scale nature of the solar wind. *Living Rev. Sol. Phys.* **16** (1), 5.

VIÑAS, A.F., GAELZER, R., MOYA, P. S., MACE, R. & ARANEDA, J.A. 2017 Linear kinetic waves in plasmas described by kappa distributions. In *Kappa Distributions*, chap. 7, pp. 329–361. Elsevier.

VIÑAS, A.F., WONG, H. K. & KLIMAS, A. J. 2000 Generation of electron suprathermal tails in the upper solar atmosphere: implications for coronal heating. *Astrophys. J.* **528** (1), 509–523.

WILSON, L.B., CHEN, L.-J., WANG, S., SCHWARTZ, S.J., TURNER, D.L., STEVENS, M.L., KASPER, J.C., OSMANE, A., CAPRIOLI, D., BALE, S.D., *et al.* 2019b Electron energy partition across interplanetary shocks. II. Statistics. *Astrophys. J. Suppl.* **245** (2), 24.

WILSON, L.B., CHEN, L.-J., WANG, S., SCHWARTZ, S.J., TURNER, D.L., STEVENS, M.L., KASPER, J.C., OSMANE, A., CAPRIOLI, D., BALE, S.D., PULUPA, M.P., SALEM, C.S. & GOODRICH, K.A. 2019*a* Electron energy partition across interplanetary shocks. I. Methodology and data product. *Astrophys. J. Suppl.* **243** (1), 8.

WILSON, L.B., KOVAL, A., SZABO, A., BRENEMAN, A., CATTELL, C.A., GOETZ, K., KELLOGG, P.J., KERSTEN, K., KASPER, J.C. & MARUCA, B.A. 2013 Electromagnetic waves and electron anisotropies downstream of supercritical interplanetary shocks. *J. Geophys. Res.: Space* **118**, 5–16.

WOODHAM, L.D., WICKS, R.T., VERSCHAREN, D., OWEN, C.J., MARUCA, B.A. & ALTERMAN, B.L. 2019 Parallel-propagating fluctuations at proton-kinetic scales in the solar wind are dominated by kinetic instabilities. *Astrophys. J*. **884** (2), L53.

YOON, P.H. 2017 Kinetic instabilities in the solar wind driven by temperature anisotropies. *Rev. Mod. Plasma Phys*. **1** (1), 4.

YOON, P.H. 2019 *Classical Kinetic Theory of Weakly Turbulent Nonlinear Plasma Processes*. Cambridge University Press.